

Agemo: an open-source library for Laplace transformed coalescence time distributions.

Gertjan Bisschop *

Institute of Evolutionary Biology, University of Edinburgh, EH9 3FL Edinburgh,
Scotland

Abstract

agemo is an open-source tool with a python API that allows users to generate the Laplace transform of the coalescence time distribution of a sample under any structured coalescent model. In addition, **agemo** provides ways to efficiently query that distribution, by using the fact that its generating function can be represented most simply as a directed graph with all possible ancestral states of the sample as nodes. Past implementations have not made full use of this, relying on computer algebra systems instead of graph traversal to process these recursive expressions. **agemo** can be used to compute the probabilities of the joint site frequency spectrum for blocks of a given size, under the specified model. Calculating these probabilities requires repeated differentiation of the generating function which suffers from an explosion in the number of terms when implemented naively. Using a closed-form expression for the coefficients of a series expansion of the equations associated with each edge, we can efficiently propagate these coefficients through the graph avoiding redundant operations.

¹ 1 Introduction

² Laplace transforms have been used extensively in coalescent theory since the introduction of the
³ structured coalescent (Takahata, 1988; Notohara, 1990; Barton and Wilson, 1995). Initially it was a

*g.bisschop@sms.ed.ac.uk

formal tool to analyse continuous-time Markov chains (Takahata, 1988; Griffiths, 1991; Wilkinson-Herbots, 1998). But as noted by Wilkinson-Herbots (1998) the Laplace transforms of the distributions of coalescence times are also interesting in their own right. The Laplace transform of a random variable has a clear probabilistic interpretation. One can think of that random variable as describing the length of an interval. If a Poisson marking process with intensity ω marks the interval, then the Laplace transform $f^*(\omega)$ is the probability of not observing any marks in the considered interval (Råde, 1972). Let the random variable be the stochastic process modelling the (sum of the) exponentially distributed waiting times describing the ancestry of a random sample, then the marking process can describe the arrival of mutations. Formulated as such, the connection to the coalescent (Kingman, 1982; Hudson, 1983; Tajima, 1983) becomes obvious, making the Laplace transform a natural choice (Weissman and Hallatschek, 2017).

Moreover, used in mathematical fields like queueing theory, the Laplace transform often provides us with an alternative description of the behaviour of a system, often simplifying its analysis in the process. In essence, this is what the generating function (GF) method as described in Lohse et al. (2011) does. Using the probabilistic interpretation of the Laplace and the fact that the transform turns convolution into multiplication (see 2.1), one can come up with a much simpler, recursive and automated, description of the distribution of the (sum of) interevent times given a set of samples and a (structured coalescent) model. Phrased differently, being given a flow diagram or coalescent state space graph describing all possible transitions during the coalescent process (see fig. 2.1.2), one can readily write down all associated expressions in the Laplace domain. This is not the case for the time domain.

This framework has been used to develop likelihood-based inference methods both for IM-type demographic histories (Lohse et al., 2011; Bunnefeld et al., 2015; Lohse et al., 2016) as well as estimating sweep parameters (Bisschop et al., 2021). Given that the GF relies on generating the coalescent state space graph, and that this state space graph will grow superexponentially with sample size, there are limitations on the sample size and number of events for which the GF can be generated and more importantly evaluated within reasonable (memory) space and time. These two bottlenecks, the ability to make mathematically tractable descriptions of a problem as well as the ability to efficiently implement the solution hold for all inference problems. The first issue is generally solved by making simplifying assumptions about recombination, either ignoring the information contained within closely linked variants completely (Gutenkunst et al., 2009; Excoffier et al., 2013), or by only ignoring recombination within very short blocks (Yang, 2002; Hey, 2004). Additionally, one can limit the description to a small number of lineages or only consider very basic underlying (demographic) models.

The second issue is often very closely connected to the type of mathematical description used.

40 In general, one will benefit from the potential to implement a particular solution in terms of data
41 structures for which efficient algorithms exist for each of the required basic operations. For example,
42 preserving matrix structure up to the point of evaluation, as used in phase-type theory (Hobolth
43 et al., 2019), will tend to have a positive impact on performance due to the existence of many
44 efficient algorithms for linear algebra operations.

45 So far, all inference approaches using the GF, rely on deriving the probability of observing each
46 of the different block-wise site frequency spectrum (bSFS) vectors. These combinations of mutation
47 configurations along the distinguished branch types within blocks of a certain length summarise the
48 joint distribution of linked polymorphisms (Bunnefeld et al., 2015). However, depending on both
49 the number of observed mutations and the number of distinguished branch types, they require re-
50 peated differentiation of the entire GF. As a consequence, any naive implementation of the GF with
51 higher-order derivatives using a computer algebra system (CAS) will quickly run into computational
52 bottlenecks, essentially limiting the extendability of the framework.

53 Previous efforts to make the framework more efficient have targeted the first bottleneck cate-
54 gory by limiting the number of distinguishable branchtypes, limiting the number of occurrences of
55 particular events, and using symmetries within the recursive description (Lohse et al., 2016). No
56 attempts have been made to tackle the second bottleneck and describe the problem in a way that
57 allows for more efficient computation.

58
59 Here we present the first open-source implementation of the GF framework and lay out the key
60 algorithms that allow us to efficiently calculate the bSFS by using the correspondence between the
61 recursive formulation of the Laplace transform and the coalescent state space graph. The focus
62 on the bSFS is only superficial however. Any future extension of the library will make use of the
63 concepts outlined here.

64 First, we will outline how the GF can be represented more succinctly. Secondly, we will lay out
65 the graph traversal algorithm allowing us to efficiently evaluate the GF. We will then apply this to
66 the bSFS by using the algorithm to propagate the coefficients of a truncated Taylor series through
67 the graph.

2 Methods

2.1 Recursive description of the Laplace transform

2.1.1 single population

Given a sample of n uniquely labelled lineages $\Omega = \{a, \dots, n\}$ coming from a single population, we can represent all possible coalescent histories of that sample as a series of trees. In each of these ranked topologies nodes represent the lineage ancestral to the subtended nodes. Alternatively, the same information can be captured by a single rooted directed graph describing the state space of all (coalescence) events affecting the history of the sampled lineages. In this graph, each node is uniquely labelled by one of the partitions of Ω . As lineages coalesce, we move through the graph from the source node, representing the set of all sampled lineages, to the root or most recent common ancestor (mrca). In the case of the neutral coalescent and a single population each path through the graph is equivalent to a single ranked topology. However, in general the state space graph will contain information on all events that affect the lineage configuration, not only those that join to lineages.

For k uncoalesced lineages, the rate of coalescence is $\binom{k}{2}$ (in units of $2N_e$ generations). Because each step is conditionally independent of the previous and as touched upon in the introduction, the Laplace transform of the sum of inter-event times or the time to the most recent common ancestor (t_{mrca}) is a simple product of all Laplace transforms of the random variable describing the waiting time to go from k to $k-1$ lineages. As such, we can associate each edge of the directed graph with a single equation describing this transition. The Laplace transform of the t_{mrca} for a single (ranked) topology can then be retrieved by multiplying the equations associated with a single path of the graph. Likewise, the entire GF is the sum of all expressions retrieved by a depth-first traversal of the graph (see 2.1.2).

Knowing that the equation associated with a single edge in the coalescent state space graph as outlined above, gives the probability of observing the coalescence event prior to any other event happening at rate ω , for any two out of k lineages, the Laplace transform is $f^*(\omega) = \frac{1}{\binom{k}{2} + \omega}$. Note that in general we can label each branch connecting two lineages in a coalescent tree by the samples that will be affected by a mutation arising during the time represented by that branch. And in general, we will associated each of these branch types with a unique dummy variable. Replacing ω by $\sum_{i=1}^b \omega_i$, we can retrieve the coalescence time distribution for each of the b distinguished branch types (Lohse et al., 2011).

2.1.2 general form

So far, we have dealt with a single population, tracking only coalescence events. In a structured population, we require at least one type of (migration) event to ensure lineages eventually all end up in the same population to allow for coalescence. These events can be incorporated in the state space graph by adding a node for each of these events and labelling that node by their impact on the tracked set of lineages. Looking at any node in the graph, the set of all possible events is determined by all outgoing edges and the set of all observable branchtypes during the time represented by each edge will be given by the label of the node from which the edges are leaving. The LT associated with a single edge still describes the probability of observing a particular event prior to all other events. So as long as the events that we have added in are associated with exponentially distributed waiting times and given that $\min(X, Y) \sim \exp(\omega_1 + \omega_2)$ when both $X \sim \exp(\omega_1)$ and $Y \sim \exp(\omega_2)$, we can still readily associate each edge with the correct equation.

$$f[\omega] = \frac{c}{\sum c_i \kappa_i + \sum l_j \lambda_j + \sum o_k \omega_k} \quad (1)$$

Here, Roman letters represent integers counting the number of ways a certain (coalescence or other) event can take place (c_i, l_j) given the current state space, or the number of branches of a particular type (o_i). The Greek letters represent the rate of the associated competing processes. Note that in the case of coalescence with multiple populations, rates are relative and given by $\kappa_i = N_{e_i}/N_{ref}$.

Each equation can be encoded as a matrix with two rows containing the integer coefficients (c, c_i, l_j, o_k). The first row represents the numerator and will only contain a single non-zero value. The second row then represents the denominator. Storing the equations this way ensures we can efficiently substitute in parameter values by taking the dot product with a vector representing a point in parameter space ($\kappa_i, \lambda_j, \omega_k$) once the Laplace transform needs to be evaluated. Also, storing equation coefficients in array form allows us to efficiently perform operations on the equations (see 2.1.4). A minimal representation of the GF therefore consists of an array containing all unique equations, and an array of arrays with equation indices describing all paths through the graph.

2.1.3 adding in events

In a structured population, we require at least one type of migration event to ensure lineages eventually all end up in the same population to allow for coalescence. Currently, two types of migration events have been implemented: uni-directional migration and mass migration. Other events can readily be incorporated by adding in a method that provides a description of what the event does to the configuration of lineages. In the state space graph, nodes are labelled as partitions

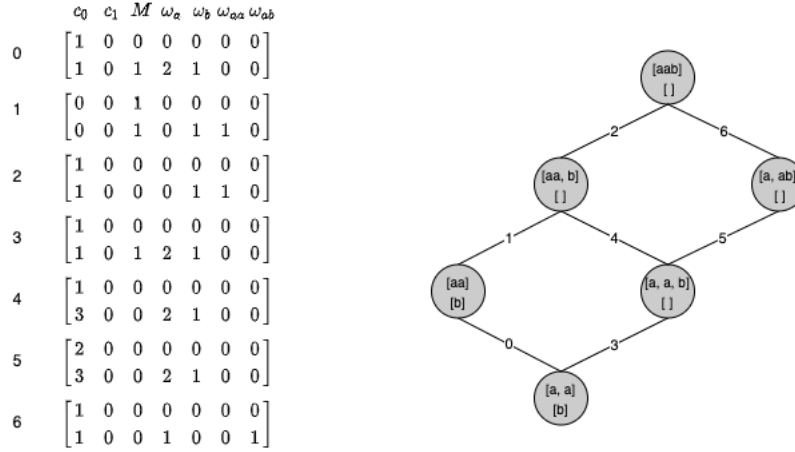


Figure 1: **From coalescent state space to equation array:** coalescent state space graph for two populations A and B with 2 and 1 unphased sample(s) respectively. The demographic model assumes a single mass migration event from population B to A back in time.

of the samples present in each of the subpopulations. One could extent this description and therefore allow for events, like mutations, that do not affect the configuration of lineages. However, there are more efficient ways of dealing with mutations (see 2.3)

Note that to limit state space size and in line with Lohse et al. (2016) migration is indeed limited to being uni-directional. Also, although both migration events are implemented as continuous exponential processes, mass migration is obviously a discrete event.

2.1.4 discrete events

Initially treating discrete events as a competing exponential process we recover the GF parametrised by the discrete time T of the event, by taking the inverse transform of the GF divided by its associated dummy variable (δ). This has been used to incorporate mass migration and bottlenecks (Lohse et al., 2011; Bunnefeld et al., 2015) as well as hard sweeps (Bisschop et al., 2021).

Previous implementations have relied on a CAS to get an analytic solution to the inverse transform. However, we can use the fact that when it comes to inverting with respect to δ each path in the graph corresponds to a product of rational functions of the form $c/(d + \delta)$ with c, d constants. And, limiting the GF to a single discrete event, all equations associated with paths departing from the node representing that event are constants with respect to delta.

Having stored all equation coefficients as an array, we can formulate a closed-form solution to

147 the inverse Laplace that allows for efficient substitution of all parameter values. Note, this means
 148 that the inverse transform does not happen until the GF is being evaluated. However, one could
 149 recover the analytical expression by providing symbolic variables to the parameter vector. This
 150 would require using a CAS like **SageMath**.

The result is a sum of terms of the form

$$C(\omega) \sum (-1)^i \frac{e^{-P_i(\omega)T}}{\prod Q_i(\omega)} \quad (2)$$

151 With P_i equalling denominator of factor i of the path, and $Q_i(\omega)$ equalling product of pairwise
 152 differences of i with all other denominators. And $C(\omega)$ the part of the path following the discrete
 153 event. The outlined correspondence between the state space graph and the GF no longer holds for
 154 the inverted GF unless we transform the graph and collapse each section of all path leading up to
 155 the discrete event node to a new node (see fig. 2.1.4). Once this operation has been performed,
 156 each path of the graph represents a product of factors again. Given that inverting is not performed
 157 until evaluation, we can simply store the indices of the equations and associate them to the edge
 158 leading up to the discrete event. Under the hood however, we perform one additional operation
 159 while collapsing the graph, and make the (sets of) equations the actual nodes of the graph (see fig.
 160 2.1.4 C). This simplifies any algorithm only dealing with the equations once generated (see 2.3).
 161 Finally, note that so far, this approach is only compatible with a single discrete event. Adding in
 162 more discrete events would require the use of a CAS to determine the inverse transform.

163 2.2 graph traversal

164 Given an equation graph (as described in fig. 2.1.4) and a dependency sequence describing the
 165 evaluation order of the graph, a general algorithm to propagate any evaluation of the equations
 166 associated with each node is given by alg. 1. It relies on the fact that implicitly the edges of the
 167 graph represent multiplication. Once both multiplication and addition have been defined for the
 168 propagated values we can rely on the commutative property to efficiently traverse the graph towards
 169 the root. Especially in the case where addition is a less costly operation than multiplication (as is
 170 the case for polynomials, see 2.3), it will pay off to add the values associated with the children of
 171 a node prior to multiplication.

172 2.3 blockwise site frequency spectrum

173 The block-wise site frequency spectrum or bSFS is the vector of site frequency spectrum counts in
 174 short blocks of a fixed length (Bunnefeld et al., 2015). It is the probability of seeing k_i mutations
 175 on each of the i distinguished branchtypes. For an unphased sample of size 3 the bSFS would be

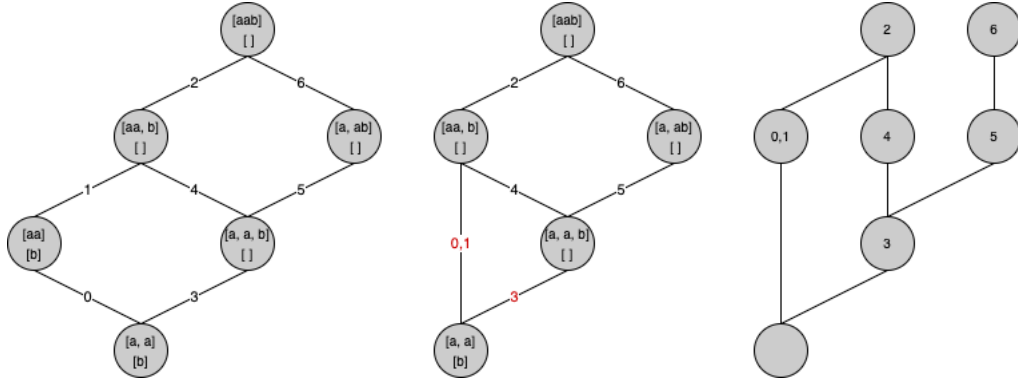


Figure 2: **From coalescent state space to equation graph:** setup identical as fig. 2.1.2. A shows the initial coalescent state space graph, while B shows the collapsed form grouping all parts of each path that require inverting with respect to the dummy variable associated with the discrete event. C takes this logic one step further turning the (sets of) equations previously associated with the edges into nodes, simplifying algorithms that do not require state space information.

Algorithm 1: Propagate values through graph.

```

1 function PROPAGATE;
   Input: adjacency list of graph, node_values, evaluation_order
2 foreach parent in evaluation_order do
3   | children = graph[parent];
4   | temp = 0;
5   | if children then
6   |   | foreach child in children do
7   |   |   | temp += node_values[child];
8   |   | end
9   |   | if parent not root then
10  |   |   | node_values[parent] = PRODUCT(temp, node_values[parent]);
11  |   | else
12  |   |   | return temp;
13  |   | end
14  | end
15 end

```

176 a vector of the form $\{k_1, k_2\}$ with k_1 and k_2 representing the number of singletons and doubletons
 177 respectively. Each count is an element within the interval $[0, 1, 2, \dots, k_{max} + 1]$ where $k_{max} + 1$ is
 178 used to bin all mutation configurations with more than k_{max} mutations.

179 Deriving the probability for each of the k_{max+2}^c possible bSFS configurations, with c the length
 180 of the bSFS vector, has thus far been the way in which the recursively generated Laplace transform
 181 of coalescence time distributions has been used. The probability for configuration \mathbf{k} is equal to
 182 $(-\theta/2)^{\sum \mathbf{k}}$ times the coefficient of $\omega^{\mathbf{k}}$ in a truncated multivariate Taylor series of the GF (see eq.
 183 (1) in Lohse et al. (2011) for details).

184 Any naive approach, based on calculating all higher order derivatives using a CAS, will suffer
 185 from an explosion in the number of terms due to the Leibniz or product rule when differentiating.
 186 Generally a CAS will fail to take into account the fact that the same partial derivatives are computed
 187 multiple times. This problem has been well-studied for the purpose of automatic differentiation
 188 algorithms (Neidinger, 1992, 1995; Griewank et al., 2000; Bettencourt et al., 2019). One possible
 189 approach to overcome this issue consists of implementing recurrence relations on how to combine
 190 truncated Taylor series. Thus essentially building higher-order derivatives from the ground up by
 191 defining the series coefficients for all elementary functions and defining the recurrence relations
 192 for arithmetic operators as well as function compositions (Neidinger, 2013). Here, we will not
 193 build up the derivatives from the elementary functions but will make use of the algorithm defining
 194 the product of two truncated Taylor series (see alg. (8) in Neidinger (2013) and, see, also adapt
 195 font). Note that adding two truncated Taylor series simply amounts to the pairwise addition of all
 196 corresponding coefficients.

Algorithm 2: Product of two truncated Taylor series (Neidinger, 2013).

```

1 function SERIES_PRODUCT;
  Input : Two same-size arrays of floats  $a$  and  $b$ 
  Output: array  $c$  of same size as  $a$  and  $b$ 
2 foreach multi-index  $\mathbf{k}$  do
3    $sum = 0$ ;
4   foreach multi-index  $\mathbf{j} \leq \mathbf{k}$  do
5      $sum = \text{ADD}(sum, a[\mathbf{j}] * b[\mathbf{k} - \mathbf{j}]);$ 
6   end
7    $c[\mathbf{k}] = sum$ ;
8 end
9 return  $c$  [ ];

```

197 Because in our case the equations associated with each of the nodes of the equations graph are
198 well characterised and fall in one of two categories depending on whether an inversion step was
199 needed, we will benefit from defining closed-form implementations of the derivatives with respect
200 to each of the distinguished branchtypes. Again, equations will either take the form of a rational
201 function with a constant numerator (branchtype variables never appear in the numerator) and a
202 multi-variate polynomial of order 1 as denominator (see eq. 1). Or will be a sum of exponentials
203 divided by higher order polynomials (see eq. 2). And for both cases, algorithms ?? and ?? respec-
204 tively show how operations on the integer coefficient matrix allow us to efficiently compute all the
205 coefficients defining a truncated Taylor series expansion of these equations ready to perform the
206 graph traversal algorithm.

207 Note however that when binning the probability of seeing more than k_{max} mutations for each
208 branchtype, a single pass through the graph does not suffice. In fact, $2^{|\mathbf{k}|}$ passes are required. This
209 is due to the fact that calculating the binned residual probabilities requires us to marginalise the
210 GF over the l variables for which the residual probability is determined. This amounts to setting
211 those l dummy variables to 0, compute all derivatives for the remaining variables and propagate
212 the coefficients of the new truncated Taylor series in $|\mathbf{k}| - l$ variables. Given that without having
213 to calculate marginals a single pass would suffice, not binning probabilities, but instead calculating
214 the probabilities of all observed mutation configuration might be more efficient in specific cases.

215 Also remark that alg. 2 contains an explicit ADD function. This refers to the fact that care
216 needs to be taken when summing (a subset of) the coefficients of a Taylor series. Because these will
217 be both positive and negative, catastrophic cancellation might occur leading to accuracy loss. We
218 have implemented the compensated summation algorithm of Ogita-Rump-Oishi (Ogita et al., 2005)
219 as an efficient way to bound the potential loss in accuracy. Another advantage of using Taylor
220 series coefficients rather than the derivatives is that the coefficients will always be smaller by a
221 factor $(\sum \mathbf{k})!$ leading to less cumulative roundoff error.

222 2.4 simplification

223 Following Lohse et al. (2016), we can simplify the GF by taking away root and/or phase information.
224 removing phase info: replacing all unique labels by a single label determined by the population they
225 were sampled from. practically: do this when providing sample list.

226 removing root: practically: pass branchtype dict, mapping branchtypes to their corresponding
227 label. How do we enforce a particular order? Otherwise, fully labelled

3 Results and Discussion

In summary, the work presented here constitutes a CAS-independent, open-source implementation of the GF. A general outline has been given on how to rely on the correspondence between the coalescent state space graph and the GF to query the distribution of Laplace transformed coalescence times efficiently. In particular, algorithms have been laid out to efficiently calculate the bSFS making this package ideal as a backend for likelihood calculations.

Currently, `agemo` is implemented in `python 3`, relying on `numba` jit-compilation to speed up the critical parts of the code. Compiling the code using `numba` has a few consequences. Firstly, compilation happens each time the code is run and will require a few seconds. This is generally not an issue given that usually many points in parameter space will be evaluated for example when calculating the bSFS. Secondly, a few of the `numpy` inbuilt numerical precision algorithms ... no longer being used following jit-compilation. This has ... us to implement a compensated sum algorithm. A better/faster solution would be to temporarily increase machine precision for the evaluation of particular sums. This is not possible using `numba` however and will require us to transfer part of the code to `C`.

Because we have opted to no longer depend on a CAS to calculate derivatives, no longer placing the evaluation order of any expression out of user's reach allowing us to alleviate potential floating point precision issues. This was not possible previously forcing any implementation to use rationals rather than floats increasing computation time. However, there might be a point whenever one might want to analyse more complex models (e.g. containing more than one discrete event) that the need for relying on symbolic algebra or automatic differentiation becomes necessary. This does not change the general idea outlined in this paper. It will still pay off to evaluate the building block equations associated with the coalescent state space graph first, and then rely on graph traversal to get to the correct results. This could be achieved by putting in place a function to propagate a user-provided array (with first dimension equal to the number of equation nodes) through the graph using user-defined addition and multiplication rules. This way, we would not have the additional burden of having a CAS as a direct dependency.

There are more efficient algorithms to multiply (truncated) multivariate polynomials. The fast Fourier transform (FFT) would allow us to perform the operation at $\mathcal{O}(n \log(n))$ with n the order of the polynomial instead of $\mathcal{O}(n^2)$ for the current multiplication. However, gains would only be noticeable for a large number of distinguished branchtypes, or a really large k_{max} values.

These algorithms will not suddenly make it possible to extent the usage of the GF to any arbitrary model and sample size. The fact remains that the number of sample configurations grows superexponentially with sample size (Lohse et al., 2016).

263

264 Any incorporate more demographic events (bottleneck,) and incorporate hard sweep approxi-
 265 mations (Bisschop et al., 2021). Although most people still process vcfs when it comes to mutation
 266 data. There is the more succinct treesequences format containing both topology information as
 267 well as mutations. It would therefore make a lot of sense to add on the ability to calculate the
 268 likelihood of a mutation configuration under a particular coalescent model as given by a marginal
 269 tree from a treesequences. This boils down to restricting the GF for that particular model to the
 270 observed topology, count the number of mutations of each distinguished branchtype and compute
 271 its probability.

272 acknowledgements

273 This work was supported by an ERC starting grant (ModelGenomLand, 757648)

274 References

- 275 Barton, N. H. and Wilson, I. (1995). Genealogies and geography. *Philosophical Transactions of the*
 276 *Royal Society B*, 349(1327):49–59.
- 277 Bettencourt, J., Johnson, M. J., and Duvenaud, B. D. (2019). Taylor-Mode Automatic Differenti-
 278 ation for Higher-Order Derivatives in JAX. 10.
- 279 Bisschop, G., Lohse, K., and Setter, D. (2021). Sweeps in time: Leveraging the joint distribution
 280 of branch lengths. *Genetics*, 219(2).
- 281 Bunnefeld, L., Frantz, L. A., and Lohse, K. (2015). Inferring bottlenecks from genome-wide samples
 282 of short sequence blocks. *Genetics*, 201(3):1157–1169.
- 283 Excoffier, L., Dupanloup, I., Huerta-Sánchez, E., Sousa, V. C., and Foll, M. (2013). Robust Demo-
 284 graphic Inference from Genomic and SNP Data. *PLoS Genetics*, 9(10).
- 285 Griewank, A., Utke, J., and Walther, A. (2000). Evaluating Higher Derivative Tensors by Forward
 286 Propagation of Univariate Taylor Series Source : Mathematics of Computation , Jul ., 2000 , Vol
 287 . 69 , No . 231 (Jul ., 2000), pp . 1117- Publi. *Mathematics of Computation*, 69(231):1117–1130.
- 288 Griffiths, R. C. (1991). The Two-Locus Ancestral Graph. *Selected proceedings of the Sheffield*
 289 *symposium on applied probability*, 18(1991):100–117.

290 Gutenkunst, R. N., Hernandez, R. D., Williamson, S. H., and Bustamante, C. D. (2009). Inferring
291 the Joint Demographic History of Multiple Populations from Multidimensional SNP Frequency
292 Data. *PLoS Genetics*, 5(10):e1000695.

293 Hey, J. (2004). Multilocus Methods for Estimating Population Sizes, Migration Rates and Diver-
294 gence Time, With Applications to the Divergence of *Drosophila pseudoobscura* and *D. persimilis*.
295 *Genetics*, 167(2):747–760.

296 Hobolth, A., Siri-Jégousse, A., and Bladt, M. (2019). Phase-type distributions in population ge-
297 netics. *Theoretical Population Biology*, 127:16–32.

298 Hudson, R. R. (1983). Testing the constant-rate neutral allele model with protein sequence data.
299 *Evolution*, 37(1):203–217.

300 Kingman, J. F. (1982). The coalescent. *Stochastic Processes and their Applications*, 13(3):235–248.

301 Lohse, K., Chmelik, M., Martin, S. H., and Barton, N. H. (2016). Efficient strategies for calculating
302 blockwise likelihoods under the coalescent. *Genetics*, 202(2):775–786.

303 Lohse, K., Harrison, R. J., and Barton, N. H. (2011). A general method for calculating likelihoods
304 under the coalescent process. *Genetics*, 189(3):977–987.

305 Neidinger, R. D. (1992). An Efficient Method for the Numerical Evaluation of Partial Derivatives
306 of Arbitrary Order. *ACM Transactions on Mathematical Software (TOMS)*, 18(2):159–173.

307 Neidinger, R. D. (1995). Computing multivariable Taylor series to arbitrary order. In *Proceedings*
308 *of the international conference on Applied programming languages - APL '95*, pages 134–144,
309 New York, New York, USA. ACM Press.

310 Neidinger, R. D. (2013). Efficient recurrence relations for univariate and multivariate Taylor series
311 coefficients. *Conference Publications*, pages 587–596.

312 Notohara, M. (1990). The coalescent and the genealogical process in geographically structured
313 population. *Journal of mathematical biology*, 29:59–75.

314 Ogita, T., Rump, S. M., and Oishi, S. (2005). Accurate sum and dot product. *SIAM Journal on*
315 *Scientific Computing*, 26(6):1955–1988.

316 Råde, L. (1972). On the use of generating functions and laplace transforms in applied probability
317 theory. *International Journal of Mathematical Education in Science and Technology*, 3(1):25–33.

318 Tajima, F. (1983). Evolutionary relationship of DNA sequences in finite populations. *Genetics*,
319 105(2):437–460.

- 320 Takahata, N. (1988). The coalescent in two partially isolated diffusion populations. *Genetical*
321 *Research*, 52(3):213–222.
- 322 Weissman, D. B. and Hallatschek, O. (2017). Minimal-assumption inference from population-
323 genomic data. *eLife*, 6:1–21.
- 324 Wilkinson-Herbots, H. M. (1998). Genealogy and subpopulation differentiation under various mod-
325 els of population structure. *Journal of Mathematical Biology*, 37(6):535–585.
- 326 Yang, Z. (2002). Likelihood and Bayes estimation of ancestral population sizes in hominoids using
327 data from multiple loci. *Genetics*, 162(4):1811–1823.

328 **Supplementary Information**

329 **closed-form derivatives**

$$\frac{\partial f(\mathbf{x})^{-1}}{\partial^{k_i} x_i} = (-1)^s s! \frac{c_i^{k_i}}{f(\mathbf{x})^2} \quad (3)$$

with $s = \sum_{i=1} k_i$ and $f(\mathbf{x}) = c_i x_i + b$

$$\frac{\partial g(\mathbf{x})}{\partial^{k_i} x_i} = c^s c_i^{k_i} g(\mathbf{x}) \quad (4)$$

330 with $s = \sum_{i=1} k_i$ and $g(\mathbf{x}) = e^{c^* \sum c_i x_i + b}$